Superalloys 2008
Roger C. Reed, Kenneth A. Green, Pierre Caron, Timothy P. Gabb, Michael G. Fahrmann, Eric S. Huron and Shiela A. Woodard
TMS (The Minerals, Metals & Materials Society), 2008

INFLUENCE OF THE γ' FRACTION ON THE γ/γ' TOPOLOGICAL INVERSION DURING HIGH TEMPERATURE CREEP OF SINGLE CRYSTAL SUPERALLOYS

P. Caron[1], C. Ramusat[1], F. Diologent[2]
[1] ONERA (Office National d'Etudes et de Recherches Aérospatiales), 29 Avenue de la Division Leclerc, F-92322 Châtillon, France
[2] Laboratoire de métallurgie mécanique, Ecole Polytechnique Fédérale de Lausanne, CH-1015 Lausanne, Switzerland

Keywords: Creep, Single Crystal, Topological inversion

Abstract

Evolution of the γ/γ' microstructure during creep at 1050°C and 150 MPa of the AM1, MC2 and MC544 single crystal superalloys was followed and quantified by evaluating the variation of the specific connectivity number of the γ' phase $N_A(\gamma')$. Complementary assessments of the γ' phase connectivity were performed on a modified MC544 alloy with a reduced amount of γ' phase and on René N6 and CMSX-10M third generation superalloys. The transition from the secondary to the tertiary creep stage is correlated to the topological inversion of the γ/γ' microstructure. The γ' phase initially surrounded by the γ phase matrix becomes progressively the connected phase as the creep deformation increases. This topological inversion occurs during creep of single crystal superalloys when the γ' phase fraction is higher than about 50% and therefore depends on the alloy chemistry and on the temperature. The γ/γ ' topological inversion occurs sooner during creep as γ ' amount increases above 50%.

Introduction

During creep of commercial nickel-based single crystal superalloys at temperatures above 900°C and under <001> tensile loading, combined effects of centrifugal stress, diffusion, γ/γ' coherency stress and γ/γ' elastic modulus misfit cause directional coalescence of strengthening γ' precipitates as rafts perpendicular to the tensile axis. The destabilisation of the rafted microstructure during the creep life can then sometimes occur through a topological inversion of the γ/γ' microstructure as explicitly reported for CMSX-4 at 950°C [1] and 1100°C [1, 2], CMSX-10 at 1100°C [2], SRR99 at 980°C [3], MC-NG at 1050°C [4, 5], Alloy 221 at 1050°C [6] and René N6 at 982°C [7]. When the γ' precipitates are initially finely dispersed in the γ matrix, the γ/γ' rafted can indeed progressively evolve such as the γ' phase completely surrounds γ phase particles. This topological inversion coincides with the onset of the accelerated creep stage which is linked to a growing activity of the deformation mechanisms in both γ and γ' phases [2-5]. However, the topological inversion does not occur for instance during creep at 1050°C of Alloy 211 [6] and CMSX-6 [1, 8]. The purpose of the present paper is therefore to focus on the evolution and stability of the γ/γ' rafted microstructure through the analysis of experimental results and published data on a series of experimental and commercial alloys and to deduce some indications for alloy selection for suited applications.

Materials

High temperature creep behaviour analysis was performed on AM1 [9] and MC2 [10] first generation superalloys, MC544 fourth generation superalloy [11] (also known as MC-NG), on a modified MC544 alloy with a reduced content of γ' phase, named MC544-LGP (Low Gamma Prime), and on René N6 [6] and CMSX-10M [12] third generation superalloys (Table 1). MC544-LGP was derived from MC544 by decreasing the contents of Al, Ti and Ta proportionately in order to reduce significantly the amount of γ' phase and by keeping almost the same γ' phase chemistry.

Small-scale laboratory heats of MC2, MC544, MC544-LGP, René N6 and CMSX-10M were melted in a high vacuum induction furnace at ONERA, while AM1 was produced by Howmet Ltd. then provided by Snecma. All single crystal rods were directionally cast at ONERA by the withdrawal process using <001> oriented seeds, except for the AM1 single crystals cast by Snecma in an industrial directional solidification furnace. The single crystal rods had orientations within 5° off a <001> direction. They were fully solution heat treated and aged using the following procedures:

- AM1: 1300°C/3h/air cooling (A.C.), 1100°C/9h/A.C., 850°C/24h/ A.C.;
- MC2: 1300°C/3h/ A.C., 1100°C/4h/ A.C., 850°C/24h/ A.C.;
- MC544 and MC544-LGP: 1310°C/3h, heating for 10 hours at a rate of $3°C.h^{-1}$, 1340°C/3h/ A.C., 1100°C/4h/ A.C., 850°C/24h/ A.C.;
- René N6: 1320°C/3h/ A.C., 1120°C/3h/ A.C., 1080°C/4h/ A.C., 900°C/4h/ A.C.;
- CMSX-10M: 1337°C/3h, heating for 10 hours at a rate of $3°C.h^{-1}$, 1367°C/3h/ A.C., 1152°C/6h/ A.C., 870°C/24h/ A.C., 760°C/30h/ A.C.

Table I. Nominal chemistries of the single crystal superalloys (wt.%)

Alloy	Ni	Co	Cr	Mo	W	Re	Ru	Al	Ti	Ta	Others
AM1	Bal.	6.5	7.8	2	5.7	-	-	5.2	1.1	7.9	-
MC2	Bal.	5	8	2	8	-	-	5	1.5	6	-
MC544	Bal.	-	4	1	5	4	4	6	0.5	5	0.1 Si; 0.1 Hf
MC544-LGP	Bal.	-	4	4	5	3	4	5.8	-	6	0.1 Si; 0.1 Hf
CMSX-10M	Bal.	1.75	2	0.4	5.4	6.5	-	5.78	0.24	8.2	0.08 Nb
René N6	Bal.	12.5	4.5	1.1	5.75	5.35	-	6	-	7.5	0.15 Hf; 0.05 C; 0.004 B

Experimental Procedures

Constant load tensile creep tests were performed in air in the temperature range 950°C-1150°C on cylindrical specimens (20 mm gauge length, 3 mm diameter) machined from fully heat treated single crystals. Creep tests were interrupted at different times at 1050°C and other ones were run to rupture at 950°C, 1050°C and 1150°C. Fully heat-treated single crystal samples were also aged for 300, 1000 and 3000 hours at 1050°C without external applied stress.

Microstructural assessments were carried out by scanning electron microscopy (SEM) using the secondary electron mode on gauge sections parallel to the stress axis of the creep specimens and on sections of the aged samples cut normal to the <001> growth axis of the single crystal rods. After mechanical polishing, the γ' phase was etched by using a mixture of 60% HCl, 15% CH_3COOH, 15% HNO_3 and 10% H_2O. The γ' phase appears in dark on all the SEM micrographs. Binary black and white images were obtained by performing a grey level threshold processing on the SEM images in order to select the γ' phase.

The microstructural changes occurring during creep and during the long-term ageing treatments were quantified by measuring the variation with time of the specific connectivity number of the γ' phase $N_A(\gamma')$ according to a procedure previously established by Fredholm [6]. The specific connectivity number of a given phase is defined as the number of particles of this phase less the number of holes contained within these particles, per area unit [13]. In the fully heat-treated γ/γ' microstructure of single crystal superalloys, $N_A(\gamma')$ is then equal to the number of γ' precipitates per area unit, i.e. the density of precipitates. In this reference state, the γ matrix is the connected phase and $N_A(\gamma')$ is positive. When the γ' phase is totally connected, $N_A(\gamma')$ is equal to one less the number of γ phase particles embedded in the γ' matrix, and is therefore negative. To quantify the γ' phase connectivity in the intermediate states, the γ' phase was skeletised and $N_A(\gamma')$ was calculated using the following expression:

$$N_A(\gamma') = (N_T - N_{TP})/2S \qquad (1)$$

where N_T is the termination number and N_{TP} the triple point number of the γ' skeleton, and S is the area of the analysed field. In the example of Figure 1, application of equation (1) gives $N_A(\gamma') = (35 - 22)/101.2 = +0.128\ \mu m^{-2}$ that means the γ' phase is still mainly embedded in the γ matrix. Topological inversion occurs when $N_A(\gamma')$ becomes negative. The topological inversion is fully achieved when all the γ particles are surrounded by the connected γ' phase.

Measurements of the γ' phase area fraction $F_A(\gamma')$ were performed by image analysis on black and white images of longitudinal sections of samples quenched after heat treatment for one hour at 1050°C, 1100°C and 1150°C. The samples were taken from specimens crept until a regular γ/γ' rafted microstructure was produced. Owing to the large lateral extension of the γ and γ' rafts, the $F_A(\gamma')$ values determined from sections normal to these platelets are considered to give a good estimation of the volume fraction of γ' phase.

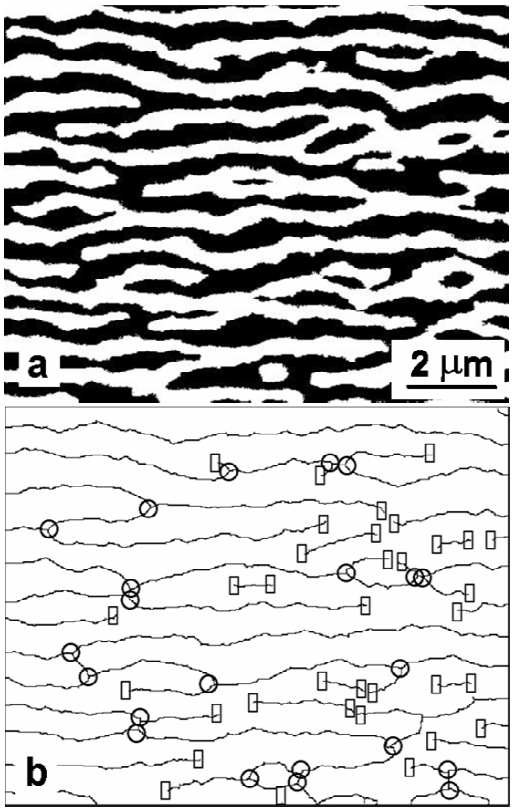

Figure 1. Image analysis of a rafted γ/γ' microstructure for the evaluation of $N_A(\gamma')$: a) binary image (γ' in black) ; b) counting of terminations (□) and triple points (○) of the γ' skeleton.

Results and Discussion

The γ/γ' microstructures in the fully heat treated conditions are shown in Figure 2. These room temperature microstructures do not illustrate accurately the situation at the onset of the creep tests because partial γ' phase solutioning occurs at these high temperatures. They allow however to compare the γ' precipitate sizes and the $N_A(\gamma')$ values in the three alloys. $N_A(\gamma')$ increases when the γ' precipitates size decreases. The γ' precipitates are the finest ones in MC544 and the largest ones in AM1.

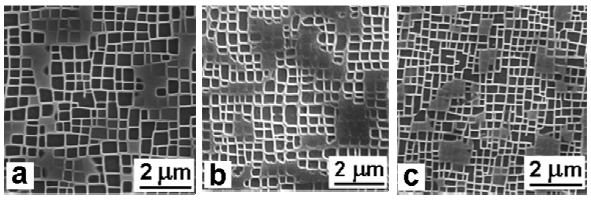

Figure 2. SEM micrographs of the γ/γ' microstructure in dendrite of fully heat-treated samples: (a) AM1, $N_A(\gamma') = +3.49\ \mu m^{-2}$; (b) MC2, $N_A(\gamma') = +6.45\ \mu m^{-2}$; (c) MC544, $N_A(\gamma') = +8.32\ \mu m^{-2}$.

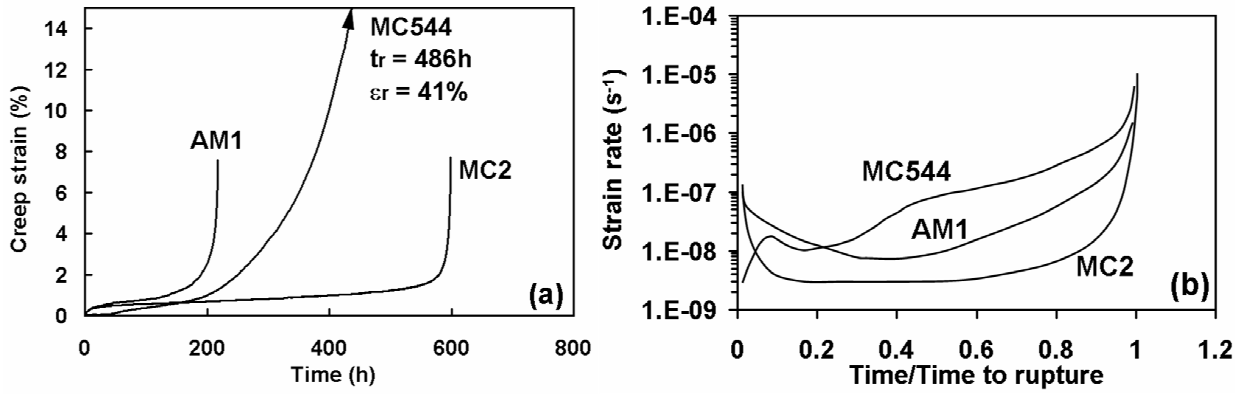

Figure 3. Typical creep curves at 1050°C and 150 MPa: (a) creep strain vs. time and (b) strain rate vs. relative time.

Typical creep curves at 1050°C and 150 MPa of the AM1, MC2 and MC544 alloys are compared in Figure 3a. The creep strain rate has been also plotted vs. relative time to highlight the differences in creep behaviour between the three superalloys and to identify more precisely the different creep stages (Figure 3b). The comparison of the creep curves evidences some differences in creep behaviour, regardless of the creep rupture life. The creep curve of MC544 is characterised by a short incubation period preceding the primary creep stage. There is no real secondary creep stage for MC544, the creep rate increasing first slowly, then faster, as soon as its minimum value is attained. A short quasi-stationary creep stage is observed for AM1 between about one-third and one-half of its creep life. The secondary creep stage occurs earlier and is significantly longer in the case of MC2.

Typical γ/γ' microstructures at increasing creep times at 1050°C are shown in Figures 4 to 6. Whereas a rafted γ/γ' microstructure normal to the <001> tensile stress axis is already established in AM1 and MC2 after only 20 hours of creep, that is not the case for MC544. The incubation period observed at the beginning of the creep curve at 1050°C of MC544 was associated to this morphological stability of the γ' precipitates and was analysed as resulting from several factors [4]. The narrower γ' channels and the higher level of solid solution strengthening of the γ matrix, as compared to AM1 and MC2, impede the movement of matrix dislocations and therefore retard the plasticization of the γ phase which was reported to enhance the rafting process [14, 15]. Moreover, the presence of rhenium in MC544 slows down all the diffusion-controlled processes and particularly the coarsening rate of the γ' precipitates, due to the very low diffusion coefficient of this alloying element [16]. In AM1 and MC2, the main microstructural evolution is then the thickening of the γ and γ' rafts which is faster in AM1. However, visual analysis of the micrographs does not permit to determine easily which the connected phase is. On the other hand, the topological inversion of the γ/γ' microstructure is clearly visible in MC544 as soon as the oriented coalescence of the γ' precipitates occurred. At the end of the creep test, coarse γ particles are completely surrounded by a γ' phase matrix, even far from the fracture surface.

The variations of $N_A(\gamma')$ with creep time are plotted in Figures 7 to 9 together with the respective creep strain rates. In AM1 and MC544, the onset of the strain rate increase corresponds to the topological inversion, i.e. to the moment at which $N_A(\gamma')$ becomes negative. This transition occurs at half of the rupture life in AM1 and already at the end of the primary creep stage in MC544. The decrease of the absolute value of $N_A(\gamma')$ in MC544 during the long stage of accelerated creep is due to the coarsening of the γ phase particles that reduces their number per unit area. In MC2, the topological inversion is observed only in the ruptured specimen and is not very pronounced, the γ and γ' phases remaining strongly interconnected.

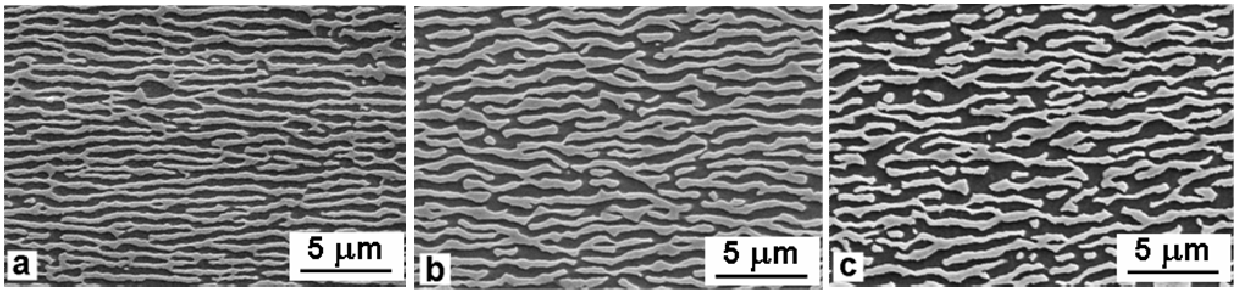

Figure 4. SEM micrographs of longitudinal sections of AM1 specimens after creep at 1050°C and 150 MPa: (a) t = 20h, $N_A(\gamma')$ = + 0.09 μm^{-2}; (b) t = 188h, $N_A(\gamma')$ = - 0.09 μm^{-2}; (c) t = 217h (rupture), $N_A(\gamma')$ = - 0.08 μm^{-2}.

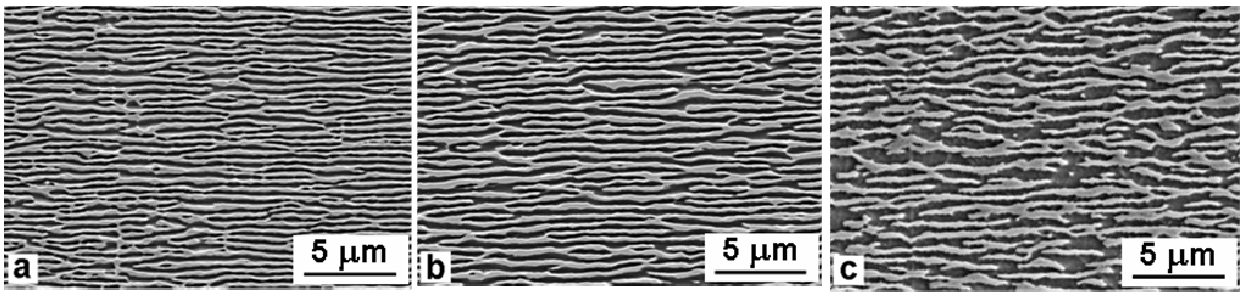

Figure 5. SEM micrographs of longitudinal sections of MC2 specimens after creep at 1050°C and 150 MPa: (a) t = 20h, $N_A(\gamma')$ = + 0.21 μm^{-2}; (b) t = 310h, $N_A(\gamma')$ = + 0.1 μm^{-2}; (c) t = 599h (rupture), $N_A(\gamma')$ = - 0.015 μm^{-2}.

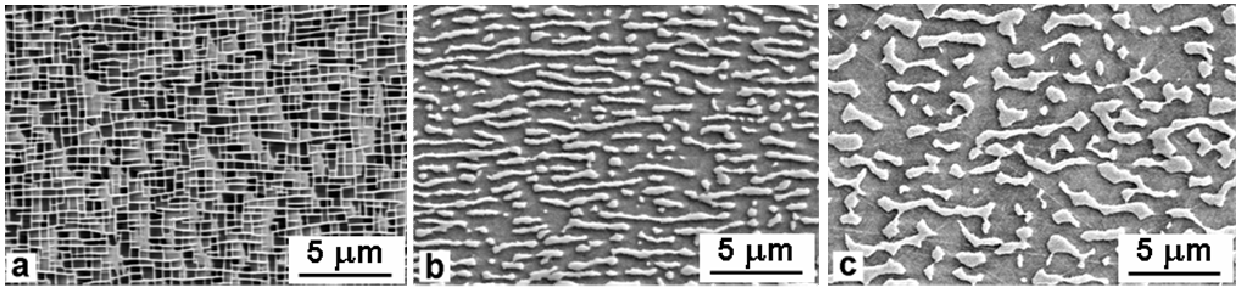

Figure 6. SEM micrographs of longitudinal sections of MC544 specimens after creep at 1050°C and 150 MPa: (a) t = 20h, $N_A(\gamma')$ = + 3.21 μm^{-2}; (b) t = 217h, $N_A(\gamma')$ = - 0.52 μm^{-2}; (c) t = 486h (rupture), $N_A(\gamma')$ = - 0.22 μm^{-2}.

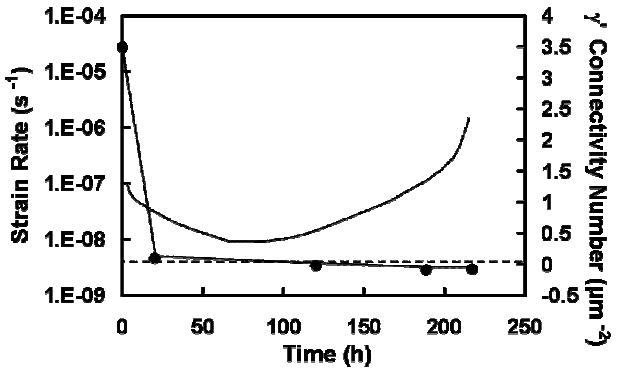

Figure 7. Evolution of $N_A(\gamma')$ during creep at 1050°C and 150 MPa of AM1.

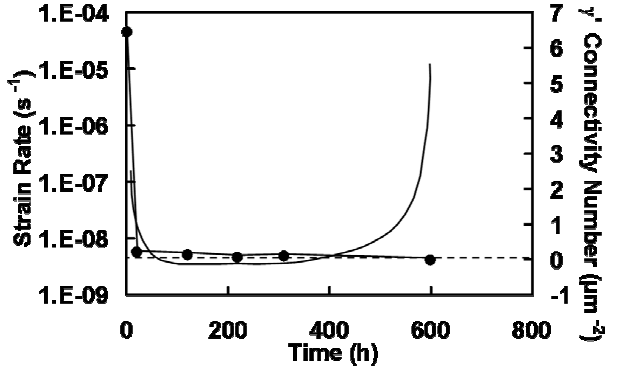

Figure 8. Evolution of $N_A(\gamma')$ during creep at 1050°C and 150 MPa of MC2.

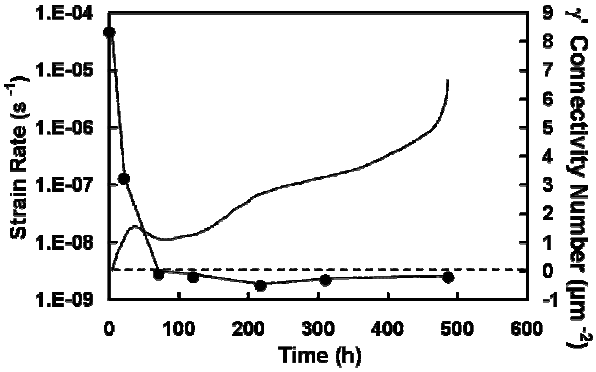

Figure 9. Evolution of $N_A(\gamma')$ during creep at 1050°C and 150 MPa of MC544.

Creep tests have been performed at 1150°C and 100 MPa on AM1, MC2 and MC544 specimens in order to check if topological inversion of the γ/γ' microstructure also occurs at very high temperature. The stress-rupture life of MC544 is dramatically longer than that of AM1 and MC2 (Figure 10). The creep curve of MC544 at 1150°C has a shape similar to that of AM1 and MC2 at 1050°C and 1150°C. There is no incubation period, a significant steady-state creep stage and a rapid tertiary stage. At this temperature, $N_A(\gamma')$ evaluation has been done only on creep ruptured specimens. For the three alloys, $N_A(\gamma')$ remains positive till the rupture that means that the γ' phase particles are always surrounded by the γ matrix at 1150°C as illustrated for MC544 in Figure 11.

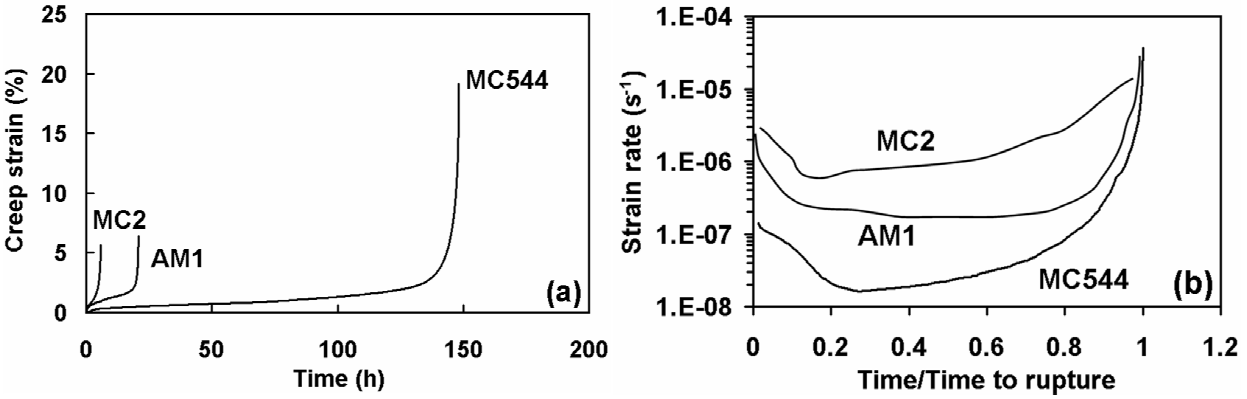

Figure 10. Typical creep curves at 1150°C and 100 MPa: (a) creep strain vs. time and (b) strain rate vs. relative time.

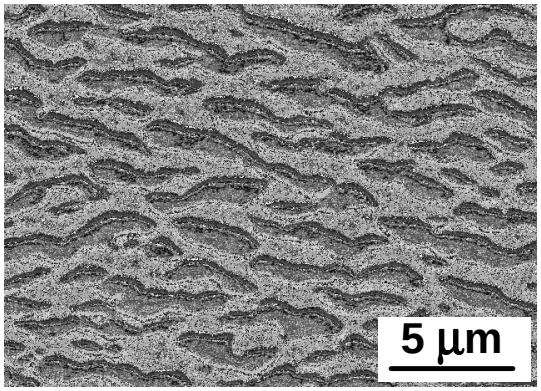

Figure 11. SEM micrograph of a longitudinal section of a MC544 specimen after rupture in creep at 1150°C and 100 MPa: $N_A(\gamma') = + 0.13\ \mu m^{-2}$. Fine γ' particles in the γ phase precipitated during cooling.

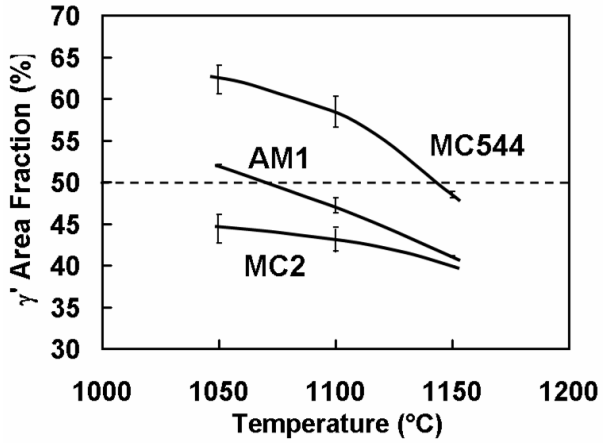

Figure 12. Variation with temperature of the γ' area fraction.

Variation with temperature in the 1050-1150°C range of the area fraction of γ' phase $F_A(\gamma')$ in AM1, MC2 and MC544 is shown in Figure 12. At 1050°C, $F_A(\gamma')$ is respectively close to 44%, 52% and 62% in MC2, AM1 and MC544. $F_A(\gamma')$ then decreases significantly when the temperature increases up to 1150°C. At 1150°C, $F_A(\gamma')$ is lower than 50% in each alloy, the higher value being always for MC544.

Supplementary microstructural assessments were performed on MC544-LGP, René N6 and CMSX-10M specimens in order to determine $F_A(\gamma')$ at 1050°C and 1150°C and $N_A(\gamma')$ at the end of creep tests at these temperatures. Such data for all the alloys of this study are compared in Table II.

These results evidence a strong relationship between the increasing amount of γ' phase and the growing tendency for topological inversion of the γ/γ' microstructure. During creep at 1050°C only MC544-LGP which contains a γ' fraction significantly lower than 50% does not experience γ/γ' topological inversion. In MC2 where the γ' fraction is higher but still lower than 50%, the γ/γ' topological inversion is observed only in the ruptured specimen. In other alloys of Table II containing more than 50% of γ' phase the topological inversion is completely achieved. Moreover, when comparing the microstructural evolutions in AM1, MC2 and MC544 alloys during creep at 1050°C, it appears that the topological inversion occurs as earlier as the γ' fraction is higher.

The temperature increase between 1050 and 1150°C leads to a decrease of $F_A(\gamma')$ to values lower than 50%, except for CMSX-10M. For all the alloys of Table II, $N_A(\gamma')$ remains positive that means that the γ' phase is once again completely surrounded by a γ phase matrix.

Table II. Area fraction of γ' phase and specific connectivity number of the γ' phase after rupture in creep at 1050°C and 150 MPa and at 1150°C and 100 MPa (nd : not determined).

	T = 1050°C		T = 1150°C	
Alloy	$F_A(\gamma')$ (%)	$N_A(\gamma')$ (μm^{-2})	$F_A(\gamma')$ (%)	$N_A(\gamma')$ (μm^{-2})
AM1	52.0	- 0.081	42.5	+ 0.105
MC2	44.5	- 0.015	39.9	+ 0.265
MC544	62.4	- 0.221	48.6	+ 0.127
MC544-LGP	40.4	+ 0.080	nd	nd
René N6	61.1	- 0.093	46.4	+ 0.133
CMSX-10M	67.3	- 0.115	55.2	+ 0.094

Topological inversion of the γ/γ' microstructure has been reported during creep at high temperatures of a number of single crystal nickel base superalloys, but often without mentioning explicitly a possible relationship with the γ' volume fraction. In other cases, this phenomenon is not outlined, whereas it is absolutely obvious when looking at the published micrographs.

Fredholm and Strudel have studied the creep behaviour at 1050°C and 140 MPa of two experimental single crystal nickel-base superalloys, Alloys 221 and 211 [6]. Rafting of the γ' phase is observed in both alloys which exhibit negative mismatch at the creep temperature. Topological inversion of the γ/γ' microstructure occurred in alloy 221 at about one third of its creep-rupture life, whereas no topological inversion occurred in alloy 211 throughout all the creep life. The content of alloying elements are the same in both alloys, except for titanium: 1.8wt.% in alloy 221 and 0.9wt.% in alloy 211. The volume fraction of γ' phase must therefore be lower in alloy 211 than in alloy 221 as confirmed by the respective values of 68 and 63% [6]. These values are significantly higher than that determined in the present study. It should be however mentioned that γ' volume fraction measurements on 221 and 211 alloys were made on γ/γ' microstructure with cuboidal γ' precipitates.

A rapid change of the sign of the γ' phase connectivity was observed during tensile creep at 950°C and 301 MPa and during creep at 1100°C and 140 MPa of <001> CMSX-4 single crystals, [1]. Such a γ/γ' topological inversion was also observed during tensile creep at 1100°C and 120 MPa of <001> CMSX-4 and CMSX-10 single crystals [2]. On the other hand, the connectivity was observed to remain positive in CMSX-6 during creep at 1050°C [1, 8]. We have measured the area fraction of γ' phase on a micrograph of a rafted CMSX-6 microstructure after creep at 1050°C, published in [8]. The resulting value of 47.5% for $F_A(\gamma')$ is coherent with the fact that no topological inversion occurs in CMSX-6 at 1050°C. Such an image analysis made on micrographs of rafted γ/γ' microstructure with a connected γ' phase in CMSX-4 taken from [17] give respective values of 53.5% and 50% at 950°C and 1100°C.

Topological inversion of the γ-γ' microstructure was also evidenced in the SRR99 single crystal alloys during tensile creep at 980°C and 200 MPa [3]. Micrographs published in [3] show clearly that the γ' fraction is significantly higher than 50% at this temperature. This phenomenon was shown to be the most pronounced at the transition from secondary to accelerated creep.

A temperature vs. time diagram was proposed for the René N6 single crystal superalloy indicating the region where γ/γ' topological inversion was observed [7]. The phenomenon occurs in the temperature range 900-1100°C, and the most rapidly around 1050°C. Topological inversion is mentioned to occurs earlier in interdendritic regions where the γ' volume fraction is higher, and does not occur above 1120°C. Both observations agree with the present results (Table II).

Topological inversion of the γ/γ' microstructure was also explicitly reported to develop after tensile creep at 1000°C and 90 MPa in the René N5, CMSX-2, CMSX-6, CMSX-11B and PWA 1483 single crystal superalloys [18]. The connectivity of the γ' phase was inferred to promote a brittle behaviour of these alloys during tensile tests in moisture at room temperature. An outcome of this study was a patent where single crystal nickel based superalloys are claimed to contain less than 50% of γ' phase in order to avoid topological inversion and therefore a loss of tensile properties in moist environment due to the brittle behaviour of the connected γ' phase [19].

Working on modified TMS-75 single crystal superalloys with various γ' volume fractions, Murakamo et al. demonstrated that the creep rupture life is the longest at 1100°C with a γ' volume fraction of 55%, that is attributed to a high stability of the rafted structure when the amounts of γ and γ' phase are nearly comparable [19]. The notion of topological inversion is however never mentioned to explain this result.

Our results, reinforced by the published results on other alloys, therefore demonstrated unambiguously that topological inversion of the γ/γ' microstructure during creep is inhibited in conditions where the fraction of γ' phase is lower than about 50%. Some small discrepancies about this transition value of the γ' fraction above which the topological inversion occurs can originate from differences in method of measurement of the γ' volume fraction by the different authors. Nevertheless, all results converge towards a value close to 50%. Moreover, in alloys where topological inversion is observed, higher is the fraction of γ' phase, earlier this phenomenon occurs during the creep life.

The relationship between γ' volume fraction and γ/γ' topological inversion can be explained by considering the total γ/γ' interface area. Once the misfit stresses relaxed by the regular networks of matrix dislocations formed at the γ/γ' interfaces, the γ' precipitate size and morphology will evolve so as to minimize the total interfacial energy. This is obtained by a reduction in γ/γ' interface area that is the driving force for diffusion controlled coarsening of the γ' particles during creep at high temperature. When the γ' volume fraction is less than 50%, this morphological evolution at constant γ' fraction leads to fewer but coarser precipitates. On the other hand, when the γ' fraction is greater than 50%, the minimization of the total γ/γ' interface area results from the topological inversion of the γ/γ' microstructure with the minor phase embedded in the major one.

Microstructural assessments of AM1 and MC544 single crystal samples aged at 1050°C for increasing durations and without external applied stress show also an evolution of the γ' phase connectivity but much slower that under creep conditions. Micrographs of Figures 13 and 14 illustrate the microstructures of AM1 and MC544 alloys in dendrite cores after ageing treatments at 1050°C for 300, 1000 and 3000 hours. In AM1 aged for 300 hours, a number of γ' precipitates have coalesced but the γ' phase is not totally connected whereas the topological inversion is fully achieved after creep for a similar duration. $N_A(\gamma')$ is still positive after 1000 hours with a value of + 0.05 and even after 3000 hours, where $N_A(\gamma')$ was measured to be – 0.003, i.e. only slightly negative, the topological inversion is not completely achieved. After 300 hours at 1050°C, the γ' precipitates have coarsened in MC544 but remains mainly cuboidal and the γ phase is still the connected phase. That is always the case after 1000 hours and 3000 hours at 1050°C, even if the γ/γ' microstructure is coarser. Clearly the microstructural evolution is slower in MC544 than in AM1 due to the rhenium addition.

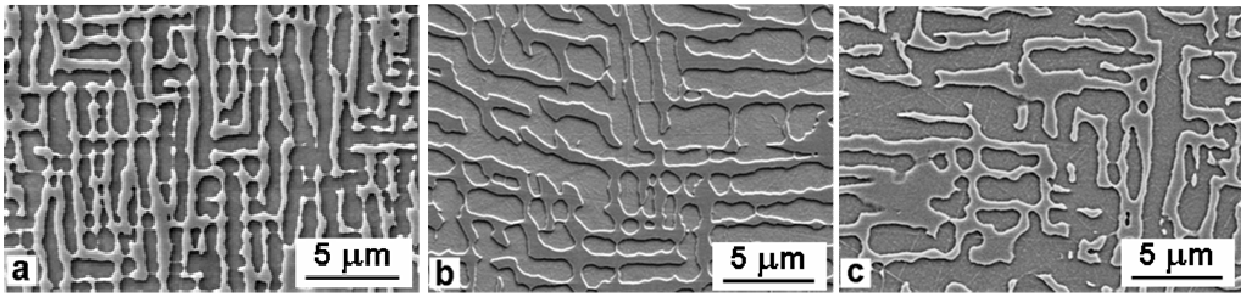

Figure 13. γ/γ' microstructure in dendrites of AM1 after long-term ageing at 1050°C : (a) 300 hours; (b) 1000 hours, $N_A(\gamma') = + 0.05\ \mu m^{-2}$; (c) 3000 hours, $N_A(\gamma') = - 0.003\ \mu m^{-2}$.

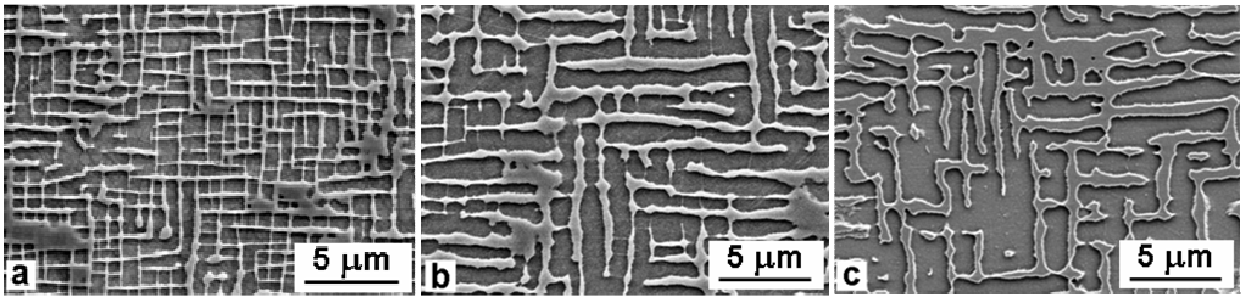

Figure 14. γ/γ' microstructure in dendrites of MC544 after long-term ageing at 1050°C : (a) 300 hours; (b) 1000 hours; (c) 3000 hours.

The applied stress which is the driving force for oriented coalescence of the γ' precipitates during creep at high temperature therefore also promotes topological inversion of the γ/γ' microstructure during creep at high temperature. Plastic strain of the γ matrix which leads to a relaxation of the coherency stresses at the γ/γ' interfaces is clearly essential for the topological inversion to operate. This hypothesis agrees with the analysis of Fredholm and Strudel who underline that the γ/γ' inversion occurs during creep of alloys containing more than 50% vol. of γ' phase whereas the γ phase still surrounds the γ' phase particles when these superalloys are heat treated without external applied stress [20].

An important issue is to evaluate the influence of the γ/γ' topological inversion on the creep behaviour. Whereas this microstructural evolution has been observed during creep in René N6 within the temperature range 900-1100°C [7] and in a Ta rich experimental alloy at 1050°C [21], the respective authors underline that this microstructural evolution does not have any detrimental effect on the high temperature creep resistance. On the contrary more recent studies highlight the accelerating effect of the topological inversion on the creep deformation rate. The deterioration of the creep resistance due to the topological inversion was thus predicted by Mughrabi on the basis of a composite model of deformation-induced internal stress [1]. Plastic deformation of the γ islands leads to a rapid increase of the deformation induced internal stress which cannot be relaxed by glide-climb motion of the γ/γ' interface dislocations. These dislocations are therefore forced to cut the γ' phase matrix. Several dislocation structure analyses have confirmed the increasing activity of the deformation mechanisms in the γ' phase when it becomes connected. High densities of faulted debris and of pairs of a/2<110> dislocations have thus been observed in MC544 after 120 hours of creep at 1050°C and 150 MPa [4, 5]. During creep at 980°C of SRR99 the topological inversion was shown to correspond to a drastic increase of the creep rate [3]. The zigzag shape of the γ/γ' interfaces in the modified microstructure is inferred to promote formation of dislocation pile-ups and consequently cutting of the γ' phase. Creep studies on CMSX-4 and CMSX-10 at 1100°C showed climb of a<100> dislocations in the connected γ' phase which in turn enables dislocation glide in the γ matrix embedded particles [2]. The topological inversion thus induces an increase of the dislocation activity in both γ and γ' phases leading to the related accelerating creep.

The stability of a rafted microstructure with a positive γ' connectivity number therefore precludes massive cutting of the γ' rafts by the γ matrix dislocations and allows to maintain a steady state creep stage during the main part of the creep life at high temperature as illustrated by the creep behaviour of MC2 at 1050°C or of MC544 at 1150°C. Comparison of creep curves where relative creep strain is plotted versus relative time highlights the similarity between the creep behaviours of MC2 at 1050°C and MC544 at 1150°C, regardless of the stress-rupture life (Figure 15). The true tertiary creep stage, which results from the combined effects of gauge section reduction, necking, initiation of cracks from the casting porosity or from the surface and so one, occurs while the γ phase is still connected, or at less while the γ and γ' phases are strongly interconnected.

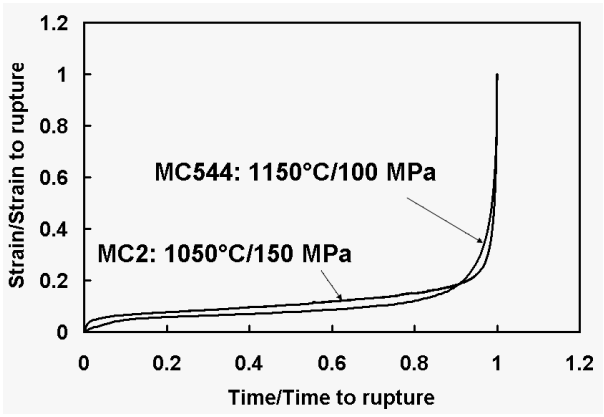

Figure 15. Comparison of the creep behaviours of MC2 at 1050°C and 150 MPa and of MC544 at 1150°C and 100 MPa.

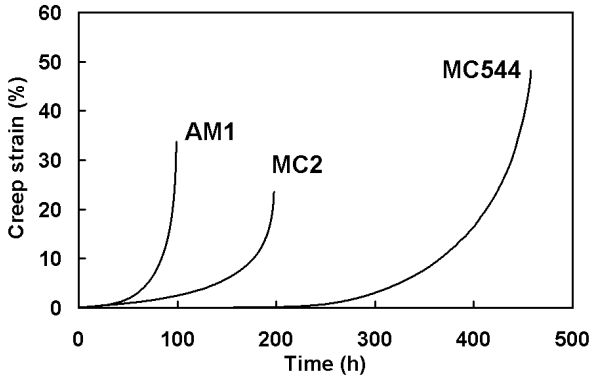

Figure 16. Typical creep curves at 950°C and 300 MPa.

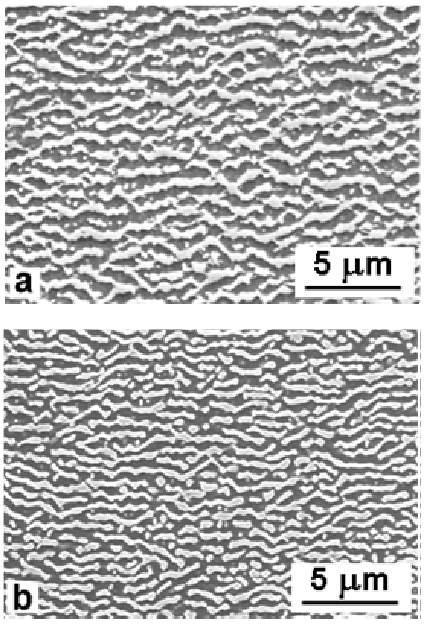

Figure 17. Inverted γ/γ' microstructure in: (a) AM1 and (b) MC544 after rupture in creep at 950°C and 300 MPa.

It should be pointed out that at 950°C and 300 MPa, the AM1, MC2 and MC544 alloys exhibit similar creep behaviours, i.e. no significant primary creep stage, no steady-state creep stage and consequently a continuous increase of the creep strain rate (Figure 16). The γ/γ' topological inversion occurs within the three alloys as shown for AM1 and MC544 in Figure 17. Whereas the γ' phase is completely connected in MC544 at the end of the creep test, the creep strength of this alloy is significantly higher than that of AM1 where some γ' particles are still embedded within the γ matrix. Depending on the alloy chemistry, the creep strength of an alloy with a fully inverted microstructure can therefore be higher than that of an alloy in which the topological inversion is not completely achieved. Presence of rhenium in MC544 offers the advantage of reducing the coarsening rate of the γ' particles due to the very low diffusion coefficient of this alloying element. The resulting γ/γ' microstructure at the end of the creep test is consequently as finer in MC544 than in AM1 although the creep rupture life is four-time longer. The γ/γ' topological inversion does not seem to be as detrimental to the creep strength as at 1050°C.

It can be pointed out that in alloys and in conditions where γ/γ' topological inversion operates continuously during the life of a single crystal component, $N_A(\gamma')$ measurements could be an efficient way to evaluate the level of microstructural damage and consequently of the residual creep life, in reference to standard microstructures generated under given creep conditions.

Some useful indications for selection or development of an alloy composition for a given application, depending on the temperature regime which must be favoured, at less as creep strength is concerned, can be drawn from the present study. A γ' phase fraction as large as possible in order to obtain a high creep strength in the very high temperature regime (T > 1100°C) is thus not favourable to the creep behaviour in the high temperature regime (1000°C < T< 1100°C) where the stability of a regular γ/γ' rafted microstructure with γ matrix surrounding γ' platelets plays a fundamental role in the creep strength of these materials. These results evidence the difficulty to design an alloy chemistry optimizing the creep strength in a very wide temperature range. Clearly, if there is no need for very high temperature creep strength, it should be better to design an alloy with a γ' fraction not higher than 50% at temperatures below 1100°C in order to preserve the connectivity of the γ phase and therefore to retards shearing of the γ' particles, and consequently precocious accelerated creep.

Conclusions

The main conclusions drawn from this study are:

1/ Topological inversion of the γ/γ' microstructure in single crystal nickel based superalloys occurs during creep at high temperature when conditions are such as the fraction of γ' phase is higher than about 50%.

2/ Comparison of the creep behaviours at 1050°C an 150 MPa of the AM1, MC2 and MC544 alloys shows that the topological inversion operates during the creep life as earlier as the γ' fraction is higher.

3/ An increase of the creep rate is associated with the γ/γ' topological inversion owing to the growing activity of dislocations in both γ and γ' phases.

4/ As alloy chemistry and temperature are the parameters which determine the γ' volume fraction, they influence the topological inversion phenomenon. This can give precious information for design or selection of alloys suited for particular creep temperature regimes.

Acknowledgements

The authors are indebted to Snecma for partial funding of this study and for providing single crystal materials.

References

1. H. Mughrabi, "γ/γ' rafting and its effect on the creep and fatigue behaviour of monocrystalline superalloys," *The Johannes Weertman Symposium*, ed. R.J. Arsenault, D. Cole, T. Gross, G. Kostorz, P.K. Liaw, S. Parameswaran, and H. Sizek (Warrendale, PA: TMS, 1996), 267-278.

2. A. Epishin, and T. Link, "Mechanisms of high-temperature creep of nickel-based superalloys under low applied stresses," *Phil. Mag*., 84 (19) (2004), 1979-2000.

3. A. Epishin, T. Link, U. Brückner, and P. Portella, "Kinetics of the topological inversion of the γ/γ'-microstructure during creep of a nickel-based superalloy," *Acta mater*., 49 (2001), 4017-4023.

4. P. Caron, M. Benyoucef, A. Coujou, J. Crestou, and N. Clément, "Creep behaviour at 1050°C of a Re-Containing Single Crystal Superalloy," *ISOMALM 2000*, ed. Baldev Raj et al. (Chennai, India: Allied Publishers Ltd.,2000), 148-156.

5. F. Diologent, P. Caron, A. Jacques, and P. Bastie, "Creep behaviour at 1050°C of a new generation single crystal superalloy," *Creep Deformation : Fundamentals and Applications*, ed. R.S. Mishra, J.C. Earthman, and S.V. Raj (Warrendale, PA: TMS, 2002), 361-370.

6. A. Fredholm, and J.-L. Strudel, "High temperature creep mechanisms in single crystals of some high performance nickel base superalloys," *High temperature Alloys, their Exploitable Potential, Proceedings of the Petten International Conference*, ed. J.B. Mariott, et al. (London, U.K.: Elsevier Applied science, 1987), 9-18.

7. W.S Walston, K.S. O'Hara, E.W. Ross, T.M. Pollock, and W.H. Murphy, "René N6: Third Generation Single Crystal Superalloy," *Superalloys 1996*, ed. R.D. Kissinger et al., (Warrendale, PA: TMS, 1996), 27-34.

8. H. Mughrabi, S. Kraft, and M. Ott, "Specific aspects of isothermal and anisothermal fatigue of the monocrystalline nickel-base superalloys CMSX-6," *Superalloys 1996*, ed. R.D. Kissinger et al., (Warrendale, PA: TMS, 1996), 335-344.

9. J.H. Davidson, A. Fredholm, T. Khan, and J.-M. Théret, French Patent N° 2557598.

10. P. Caron, and T. Khan, "Development of a New Nickel Based Single Crystal Turbine Blade Alloy for Very High Temperatures," *Advanced Materials and Processes, Vol. 1*, ed. H.E. Exner and V. Schumacher (Oberursel, Germany: DGM Informationsgesellschaft mbH, 1990), 333-338.

11. P. Caron, "High γ' Solvus New Generation Nickel-Based Superalloys for Single Crystal Turbine Blade Applications," *Superalloys 2000*, ed. T.M. Pollock, et al. (Warrendale, PA: TMS, 2000), 737-746.

12. G.L. Erickson., "The Development and Application of CMSX-10," *Superalloys 1996*, ed. R.D. Kissinger et al. (Warrendale, PA: The Minerals, Metals & Materials Society, 1996), 35-44.

13. M. Coster, and J.-L. Chermant, *Précis d'analyse d'images* (Paris, France: Presses du CNRS, 1989), 23.

14. T.M. Pollock, and A.S. Argon, "Directional coarsening in nickel-base single crystals with high volume fractions of coherent precipitates," *Acta metal. Mater.*, 42 (1994), 195-205.

15. N. Matan, D.C. Cox, C.M. Rae, and R.C. Reed, "On the kinetics of rafting in CMSX-4 superalloy single crystals," *Acta mater*., 47 (1999), 2031-2045.

16. M. Karunaratne, P. Carter, and R.C. Reed, "Interdiffusion in the face-centred cubic phase of the Ni-Re, Ni-Ta and Ni-W systems between 900 and 1300°C," *Mater. Sc. Eng.*, A281 (2000), 229-233.

17. H. Mughrabi, W. Schneider, V. Sass, and C. Lang, "The effect of raft formation on the high-temperature creep deformation behaviour of the monocrystalline nickel-base superalloy CMSX-4," *Strength of Materials, ICSMA 10*, ed. H. Oikawa et al. (Sendai, Japan: The Japan institute of Metals, 1992), 705-708.

18. M. Nazmy, A. Künzler, J. Denk, and R. Baumann, "The effect of strain rate on the room temperature tensile properties of single crystal superalloys," *Scripta materialia*, 47 (2002), 521-525.

19. R. Baumann, D. Duhl, A. Kuenzler, and M. Nazmy, "Nickel-base superalloy," US patent # 6,706,241, 2004.

20. T. Murakamo, T. Kobayashi, Y. Koizumi, and H. Harada, "Creep behaviour of Ni-base single-crystal superalloys with various γ' volume fraction," *Acta Materialia*, 52 (2004) 3737-3744.

21. A. Fredholm, and J.-L. Strudel, "On the creep resistance of some nickel base single crystals," *Superalloys 1984*, ed. M. Gell et al. (Warrendale, PA: The Metallurgical Society of AIME, 1984), 211-220.